

# Stability of the thermohaline circulation in a simple coupled model

By GERRIT LOHMANN<sup>\*1</sup>, RÜDIGER GERDES<sup>1</sup> and DELIANG CHEN<sup>2</sup>, <sup>1</sup>*Alfred-Wegener-Institute for Polar and Marine Research, Am Handelshafen 12, D-27570 Bremerhaven, Germany;*  
<sup>2</sup>*Department of Physical Geography, Earth Sciences Centre, Göteborg University, Göteborg, Sweden*

(Manuscript received 8 February 1995; in final form 16 October 1995)

## ABSTRACT

In an analytical study, the stability of the thermohaline circulation with respect to freshwater perturbations in high latitudes is investigated. The study is based on a coupled ocean and atmosphere box model in an idealized North Atlantic geometry. The box model provides a qualitative understanding of how the thermohaline circulation is affected by feedback mechanisms associated with changes in atmospheric transports of heat and moisture. Within a linear analysis, we examine the stability of the thermohaline circulation for a range of different atmospheric boundary conditions. The stability of the coupled system depends on the imposed transport parameterizations and the basic state. For the underlying non-linear system, we examine the sensitivity with respect to the strength of salinity perturbation.

## 1. Introduction

The oceanic thermohaline circulation (THC) is a major component of the climate system, transporting heat and salt poleward. The circulation is driven by horizontal buoyancy gradients that result from surface fluxes of heat and fresh water. The fluxes affect oceanic surface salinity and temperature in different ways: Local sea surface temperature anomalies are quickly removed by a coupling between the ocean surface and the atmospheric boundary layer through sensible and latent heat fluxes, whereas there is no corresponding mechanism for sea surface salinity anomalies. A recent anomaly in surface salinity of the northern North Atlantic, the Great Salinity Anomaly (GSA), could thus persist for more than a decade (Dickson et al., 1988).

Perturbations of the meridional transport in the ocean can be amplified by a positive feedback in the salt transport. A weaker northward salt transport brings less dense water to high latitudes, which further reduces the meridional transport. It is of interest to know which processes determine the stability of today's "salinity conveyor belt" (Broecker and Peng, 1989), which is characterized by strong poleward heat and salt transports in the North Atlantic. Paleoclimate studies suggest that changes in the THC are linked to meltwater events originating from retreating glaciers of the Barents shelf and North America (Keigwin et al., 1991). High-resolution records from the deep western basin of the North Atlantic suggest that reduced North Atlantic deep water formation was associated with a meltwater input 16 900–17 100 years B.P. (Sarnthein et al., 1994).

Many investigators analyzing the stability of the THC prescribe the atmospheric temperature and fresh water flux at the ocean surface (mixed boundary conditions). These ocean models cannot correctly describe the sensitivity of the coupled

\* Corresponding author, current affiliation: Max-Planck-Institute for Meteorology, Bundesstr. 55, D-20146 Hamburg, Germany.  
email: gerrit.Lohmann@dkrz.de

atmosphere-ocean system because important feedbacks are neglected. Experiments with changed heat flux parameterizations (Stocker et al., 1992; Zhang et al., 1993; Rahmstorf and Willebrand, 1995) show a more stable THC. Changes in the surface salinity will affect the heat loss of the ocean, which influences the local air temperature and radiation balance. This in turn causes changes in the atmospheric transports of heat and moisture and in the oceanic heat and salt transports intern.

Two recent studies have shown that the meridional transports of heat and moisture in the atmosphere do influence the stability of the THC. Lohmann et al. (1995) coupled a three-dimensional ocean general circulation model to an atmospheric energy balance model (EBM) and found that the atmospheric heat transport is the most important atmospheric destabilizing feedback, partly compensating for the stabilizing effect of finite atmospheric heat capacity. Nakamura et al. (1994) used a box model and concluded that the change in fresh water flux is the dominating destabilizing feedback.

In this study, we investigate analytically the feedbacks affecting the THC. A box model approach is used, as it is considered the most simple atmosphere-ocean system. The stability properties of our simplified system should be seen as only a rough estimate of the sensitivity of a more realistic circulation. However, feedbacks related to the transport of salt, heat and moisture in our box model are thought to qualitatively reflect the processes weakening the THC through freshening events at high latitudes, such as the GSA and meltwater events. In Section 2, the model components will be presented. The stability of the THC in the North Atlantic is assessed by a linear stability analysis in Section 3. The amount of salinity perturbation causing a breakdown of the non-linear coupled system is estimated numerically. Our conclusions are given in Section 4.

## 2. Model

The box model consists of two boxes for the upper ocean and two boxes for the atmosphere. The geometry of the model (Fig. 1) mimics the North Atlantic, with an ocean box at low latitudes ranging from the equator to 40°N, and a high latitude box between 40° and 70°N. Both upper

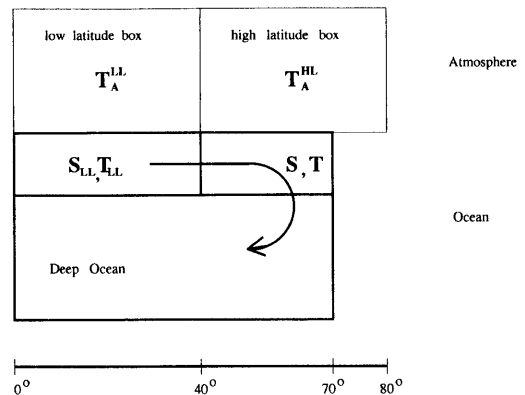


Fig. 1. Schematic representation of the model configuration.

ocean boxes are 100 m thick. The atmosphere is vertically integrated and consists of a low latitude box ranging from the equator to 40° North and a high latitude box between 40°N and 80°N. A deep ocean box with a depth of 4000 m completes the model.

### 2.1. Ocean model

In the North Atlantic, both surface temperature and salinity decrease with increasing latitudes. We denote  $\Delta T = T - T_{LL} < 0$  and  $\Delta S = S - S_{LL} < 0$  as the differences in oceanic temperature and salinity between the high latitude and the low latitude boxes. The heat and salt balances are parameterized similar to Stommel's box model (1961, 1993). Maas (1994) has shown that the dynamics of Stommel's box model can be derived rigorously from vorticity equations. The non-linear equations for temperature  $T$  and salinity  $S$  for the high latitude box are:

$$\frac{d}{dt} T = -\frac{\Phi}{V} \Delta T - \frac{F_{oa}}{\rho_o c_p \Delta z}, \quad (1)$$

$$\frac{d}{dt} S = -\frac{\Phi}{V} \Delta S - \frac{S_o}{\Delta z} (P - E), \quad (2)$$

where  $V$  is the volume of that box,  $(P - E)$  denotes precipitation minus evaporation,  $F_{oa}$  is the heat flux at the ocean-atmosphere interface, and  $S_o$  is a reference salinity of 35 psu. The heat capacity of the ocean layer that interacts with the atmosphere is  $\rho_o c_p \Delta z$  with  $\Delta z = 100$  m, the thickness of the

upper ocean boxes. The overturning rate  $\Phi$  is assumed to be proportional to the meridional density difference:

$$\Phi = -c(\alpha\Delta T - \beta\Delta S), \quad (3)$$

where  $\alpha = 0.15 \text{ K}^{-1}$  and  $0.8 \text{ psu}^{-1}$  and the thermal and haline expansion coefficients, respectively, and  $c = 17 \cdot 10^6 \text{ m}^3 \text{ s}^{-1}$  is a tunable parameter that is used to reproduce the present meridional overturning in the Atlantic. The overturning rate  $\Phi$  must be positive, otherwise (1, 2) do not apply. This is no restriction as long as we consider only today's circulation with cold water sinking at high latitudes. All water transported poleward will be brought to the deep ocean at high latitudes. Therefore, the density of the deep ocean box  $\rho_D$  is determined by

$$\frac{d}{dt} \rho_D = -\frac{\Phi}{V_D} (\rho_D - \rho), \quad (4)$$

where  $V_D$  and  $\rho$  are the volume of the deep ocean box and the density of the high latitude box, respectively. The density of the deep ocean box relaxes towards the high latitude density  $\rho$  with the long time constant  $\Phi^{-1} V_D$ . Reducing the high latitude density, statically instability does not occur whereas an increased  $\rho$  requires convective mixing to prevent statically unstable solutions.

Restoring the salinity to a climatological value  $S^*$ , the expression  $(S_0/\Delta z)(P - E)$  in eq. (2) must be substituted by  $(1/\tau)(S - S^*)$  with an arbitrary time constant  $\tau$  (often chosen to be about one month).

The heat flux between the ocean and atmosphere is calculated by a linearized bulk formula:

$$F_{\text{oa}} = Q_1 + Q_2(T - T_A), \quad (5)$$

with  $Q_1 = -50 \text{ W m}^{-2}$  and  $Q_2 = 38 \text{ W m}^{-2} \text{ K}^{-1}$  for the high latitude box (Oort and Peixoto, 1983; Oberhuber, 1988).

## 2.2. Atmosphere model

For our analytical investigation we seek an atmospheric model that is embedded in the class of linear models defined by Bretherton (1982). We start from the stationary vertically integrated balances of heat and water vapour mixing ratio  $q$ :

$$\int \frac{dp}{g} \nabla \cdot (C_p v T_a) + \int \frac{dp}{g} \nabla \cdot (L_v v q)$$

$$= Q_R^t - Q_R^b + L_v E + Q_s$$

$$= Q_R^t + F_{\text{oa}}, \quad (6)$$

$$\int \frac{dp}{g} \nabla \cdot (L_v v q) = L_v (E - P), \quad (7)$$

where  $T_a$  is the atmospheric temperature at pressure  $p$ ,  $Q_s$  is the sensible heat flux at the ground,  $Q_R^t$  and  $Q_R^b$  are the net radiation at the top and at the bottom of the atmosphere, and  $g$  is the acceleration due to gravity. The transport terms contain the atmospheric heat capacity  $C_p$ , the latent heat of condensation  $L_v$  and the meridional velocity  $v$ . A linear relation is applied for the outgoing long-wave radiation (Chen et al., 1995):  $A + BT_A$  with  $A = 220 \text{ W m}^{-2}$  and  $B = 2 \text{ W m}^{-2} \text{ K}^{-1}$ .

In the box model, the transport terms apply to the border between low and high latitude boxes at  $\phi_0 = 40^\circ \text{N}$ . The poleward transport of heat and water vapour due to the mean circulation and stationary eddies are assumed constant in time. A parameterization of the transient eddies in terms of the mean meridional temperature gradient can be based on the theory of baroclinic instability (Green, 1970; Branscome, 1983). These theoretical parameterizations have been tested in statistical dynamical models by Vallis (1982) and Stone and Yao (1990). Stone and Miller (1980) derived an empirical relationship between the mean meridional temperature gradient and the sensible heat transport by stationary and transient eddies. They found an approximately quadratic power law for middle latitudes, which is consistent with the theoretical parameterizations.

For the fluxes of water vapour, we follow Stone and Yao (1990) and assume a constant relative humidity  $rh$ , so that the mixing ratio of water vapour  $q$  can be expressed as  $q = rh q_s$ , where  $q_s$  is the saturation mixing ratio. As in Chen et al. (1995) we relate the transport terms to the mean temperature gradient at the surface.

$$F_s = \int \frac{dp}{g} C_p v' T'_a = K_s^{(r)} \left| \frac{\partial T_A}{\partial y} \right|', \quad (8)$$

$$F_l = \int \frac{dp}{g} L_v v' q' = K_l^{(r)} L_v rh(p_0) \frac{\partial q_s(p_0, T_A)}{\partial T_A} \left| \frac{\partial T_A}{\partial y} \right|', \quad (9)$$

where ' denotes the deviations from the climatological mean quantities,  $K_s^{(r)}$  and  $K_l^{(r)}$  are the

diffusion coefficients for the sensible and latent heat transport associated with power  $r$ .  $T_A$  is the atmospheric temperature at  $p_0 = 1000$  mb.

We consider an ocean basin which occupies a sector covering  $1/5$  of the total zonal area. The catchment area for the fresh water flux and the portion of the eddy heat transports relevant for our model is assumed somewhat larger at  $1/3$  of the zonal area.

To keep the atmospheric model analytically tractable, we expand (8) and (9) around the climatological transport and retain only the linear terms:

$$\delta F_s = r K_s^{(1)} \left| \frac{\partial(\delta T_A)}{\partial y} \right|, \quad (10)$$

$$\delta F_l = K_l^{(r)} r h L_v \left\{ r \left( \frac{\partial q_s}{\partial T_A} \right)_0 \left| \frac{\partial T_A}{\partial y} \right|_0^{r-1} \left| \frac{\partial(\delta T_A)}{\partial y} \right| + \left| \frac{\partial T_A}{\partial y} \right|_0^r \left( \frac{\partial^2 q_s}{\partial T_A^2} \right)_0 \delta T_A \right\}, \quad (11)$$

where subscripts  $(\dots)_0$  and  $\delta$  indicate climatological values and deviations, respectively. To derive (10), we used the definition

$$K_s^{(r)} = (F_s)_0 \left| \frac{\partial T_A}{\partial y} \right|_0^{-r} = K_s^{(1)} \left| \frac{\partial T_A}{\partial y} \right|_0^{-r+1}.$$

The diffusion coefficients are estimated from observed eddy heat transports and temperatures (Oort and Peixoto, 1983). With a sensible heat transport of 2.5 PW, and a temperature difference of 30 K over  $60^\circ$  latitude, we arrive at  $K_s^{(1)} = 0.05$  PW K $^{-1}$  for the sensible eddy heat transport. As for the sensible heat transport in eq. (10), the 2nd term on the right hand side in (11) gives a factor  $r$ , whereas the variation of the first term in (11) is independent of  $r$ . Therefore, the anomalous latent eddy heat transport in our linear model can be written as

$$\delta F_l = r K_{l0}^{(1)} \left| \frac{\partial(\delta T_A)}{\partial y} \right| - K_{l1} \delta T_A. \quad (12)$$

From Oort and Peixoto (1983) and Bolton (1980) we estimate the coefficients  $K_{l0}^{(1)}$  to be  $0.03$  PW K $^{-1}$  and  $K_{l1}$  to be  $7.8 \cdot 10^6$  W K $^{-1}$  m $^{-1}$ . The dependence of the stability of the THC on the strength and the parameterization of the transient transports in this model is investigated in Section 3.

At  $80^\circ$ N, we assume vanishing eddy moisture

transport. Changes of fresh water flux at high latitudes are therefore determined by changes in temperature and temperature gradient at  $\phi_0$ . Using (7) and (12), we get

$$L_v \delta(P - E) = \frac{1}{L_y} \delta \left( \int \frac{dp}{g} L_v v q \right) (\phi_0) \quad (13)$$

$$= r K_{l0}^{(1)} \left| \frac{\partial(\delta T_A)}{\partial y} \right| - K_{l1} \delta T_A(\phi_0), \quad (14)$$

where  $L_y$  is the grid distance of the atmospheric model. The temperature at  $\phi_0$  is the average of low and high latitude atmospheric boxes:

$$T_A(\phi_0) = \frac{T_A^{\text{HL}} + T_A^{\text{LL}}}{2}.$$

Fresh water exchanges of the North Atlantic basin with other basins are neglected. This has been estimated for the North Atlantic (north of  $24^\circ$ ) as a volume loss of  $0.03 \cdot 10^6$  m $^2$  s $^{-1}$  with an atmosphere general circulation model (Zaucker and Broecker, 1992). There is a great uncertainty in these estimates. However, the climate system can be very sensitive to the zonal transport of water vapour, which has been shown by Birchfield (1989) and Stocker et al. (1992).

### 2.3. Coupled system

In analyzing the stability of the coupled system subject to salinity perturbations at high latitudes, we assume a time scale separation. Local processes at high latitudes associated with changed sinking rates act on a much shorter time scale than the large-scale advection affecting the low latitude temperature and salinity. Therefore, as a first order approximation, salinities and temperatures at low latitudes and for the deep ocean are held constant. This assumption is appropriate as long as the volumes of the surface layer boxes are smaller than the deep ocean box and other possible equilibria of (1, 2) are not considered.

Assuming constant oceanic temperature at low latitudes, changes of the low latitude atmospheric temperature can be expressed by the high latitude atmospheric temperature using the energy balance (6):

$$\delta T_a^{\text{LL}} = \frac{K}{K + B + Q_2^{\text{LL}}} \delta T_a^{\text{HL}} = \eta \delta T_a^{\text{HL}}, \quad (15)$$

where  $Q_2^{\text{LL}}$  is the heat flux rate at low latitudes,

chosen as  $50 \text{ Wm}^{-2} \text{ K}^{-1}$  (Oberhuber, 1988). We define a transport parameter  $K$  for the atmospheric heat transport as:

$$K = \frac{1}{L_y} \left( r \frac{K_s^{(1)} + K_{10}^{(1)}}{L_y} \pm \frac{K_{11}}{2} \right). \quad (16)$$

The term  $\pm K_{11}/2$  results from the temperature dependence of the latent heat transport in (12). The negative sign (reduced transport) applies for negative temperature anomalies  $\delta T_a^{\text{HL}}$ . At high latitudes with our chosen model geometry, the area of the atmospheric box is 1.9 times larger than the oceanic box. From (14) and (15), we arrive for the change in surface fresh water flux at  $\delta(P - E)$

$$= -1.9 \frac{r K_{10}^{(1)} (1 - \eta)/L_y \pm K_{11} (1 + \eta)/2}{L_y L_v \rho_w} \delta T_a^{\text{HL}} \quad (17)$$

$$= -K_2 \delta T_a^{\text{HL}}, \quad (18)$$

where  $\rho_w$  is the density of fresh water and  $K_2$  is a sensitivity coefficient of the hydrological cycle.

For simplicity we consider from now on only negative temperature anomalies, and therefore, only the minus signs in eqs. (16, 18) are used. For this case and for  $r = 1$ , the parameters  $K$ ,  $K_2$  and  $\eta$  are:  $K = 3.2 \text{ Wm}^{-2} \text{ K}^{-1}$ ,  $K_2 = 12 \text{ mm yr}^{-1} \text{ K}^{-1}$  and  $\eta = 0.06$  using the estimates for  $K_s^{(1)}$ ,  $K_{10}^{(1)}$  and  $K_{11}$  specified above. The small value of  $\eta$  means that the low latitude response is only a small fraction of the atmospheric anomaly at high latitudes.

Choosing a basic state  $(\Delta T^0, \Delta S^0) = (-13.5 \text{ K}, -1.5 \text{ psu})$ , we calculate the equilibrium stream function  $\Phi^0 = 14 \cdot 10^6 \text{ m}^3 \text{ s}^{-1}$  and the equilibrium fresh water flux for the high latitude oceanic box,

$$(P - E)^0 = -\frac{\Delta z}{S_0} \frac{\Phi^0}{V} \Delta S^0 = 1.25 \text{ m yr}^{-1}$$

which corresponds to a fresh water flux of  $0.65 \text{ m yr}^{-1}$  for the high latitude atmospheric box. Both, stream function and fresh water flux, are typical for the present climate (Dickson and Brown, 1994; Oort and Peixoto, 1983). Subtracting the basic state from (1) and (2) yields a set of non-linear differential equations for the perturbations  $\Delta T' = \Delta T - \Delta T^0$  and  $\Delta S' = \Delta S - \Delta S^0$ :

$$\frac{d}{dt} \Delta T' = -\frac{\Phi^0}{V} \Delta T' - \frac{\Phi'}{V} \Delta T' - \frac{\Phi'}{V} \Delta T^0$$

$$-\frac{F'_{\text{oa}}}{\rho_0 c_o \Delta z}, \quad (19)$$

$$\begin{aligned} \frac{d}{dt} \Delta S' = & -\frac{\Phi^0}{V} \Delta S' - \frac{\Phi'}{V} \Delta S' - \frac{\Phi'}{V} \Delta S^0 \\ & + \frac{S_0}{\Delta z} K_2 \delta T_a^{\text{HL}}. \end{aligned} \quad (20)$$

The deviation from the equilibrium atmosphere-ocean heat flux,  $F'_{\text{oa}}$ , and fresh water flux,  $K_2 \delta T_a^{\text{HL}}$ , depend on the formulation of the atmosphere model. Making the substitution

$$\varepsilon = \frac{\delta T_a^{\text{HL}}}{\Delta T'},$$

$F'_{\text{oa}}$  can be written as

$$F'_{\text{oa}} = (1 - \varepsilon) Q_2 \Delta T'. \quad (21)$$

The surface fresh water flux term in (20) becomes

$$\frac{S_0}{\Delta z} K_2 \delta T_a^{\text{HL}} = \frac{S_0}{\Delta z} K_2 \varepsilon \Delta T'.$$

In the case of a restoring boundary condition, this term has to be substituted for, by  $-(1/\tau) \Delta S'$ , which effectively removes sea surface salinity anomalies.

Different representations of the atmospheric heat transport are now reduced to different values of  $\varepsilon$ . The parameter  $\varepsilon$  is calculated from the temperature equation (6):

$$\varepsilon = \frac{Q_2}{Q_2 + B + K(1 - \eta)}. \quad (22)$$

For a fixed atmospheric temperature, as with mixed boundary conditions,  $\varepsilon$  is zero. For a variable atmospheric temperature,  $\varepsilon$  is greater than zero and  $\varepsilon$  is maximal if no anomalous atmospheric transport is allowed:

$$\varepsilon_{\text{max}} = \frac{Q_2}{Q_2 + B} \approx 0.94.$$

In the coupled system with  $r = 1$  and the estimated  $K_s^{(1)}$ ,  $K_{10}^{(1)}$ ,  $K_{11}$ , the value of  $\varepsilon$  is

$$\varepsilon = \frac{Q_2}{Q_2 + B + K(1 - \eta)} \approx 0.88. \quad (23)$$

The anomalous heat loss from the ocean to the atmosphere,  $F'_{\text{oa}}$ , strongly determines the gain of potential energy in the ocean and therefore deep

water formation at high latitudes. With the notation introduced above (21) yields a typical time scale

$$\lambda = \frac{1}{(1 - \varepsilon)} \frac{\rho_0 c_p \Delta z}{Q_2}, \quad (24)$$

for the time it takes to remove sea surface temperature anomalies. A relatively short time scale (with  $\varepsilon = 0$ ) describes the local ocean-atmosphere heat exchange (Haney, 1971). Several authors (Zhang et al., 1993; Mikolajewicz and Maier-Reimer, 1994; Power and Kleeman, 1994), modified the mixed boundary conditions and varied this time scale by reducing the relaxation constant  $Q_2$  to  $Q'_2$ . In the frame work of our box model it is convenient to recast this in terms of an equivalent  $\varepsilon_{\text{equiv}}$ , defined by

$$Q'_2 = Q_2(1 - \varepsilon_{\text{equiv}}). \quad (25)$$

With  $\varepsilon_{\text{equiv}} > 0$ , they found a reduced sensitivity of the THC. We will discuss the implication of the time scale for the stability of the THC in Section 3. The question is under what kind of atmosphere the system remains stable subject to perturbations of salinity at high latitudes.

### 3. Stability analysis

Mathematically, the linear stability analysis of the equilibrium ( $\Delta T^0$ ,  $\Delta S^0$ ) can be reduced to the question of whether the determinant of the linear terms of eqs. (19, 20) is positive. After a little algebraic manipulation one can write the stability condition as:

$\varepsilon >$

$$\left[ -\frac{S_0 K_2}{\Delta z} \frac{c\beta}{V} \Delta T^0 + \frac{Q_2}{\rho_0 c_p \Delta z} \left( \frac{\Phi^0}{V} + \frac{c\beta}{V} \Delta S^0 \right) \right]^{-1} \times \left\{ \frac{Q_2}{\rho_0 c_p \Delta z} \left( \frac{\Phi^0}{V} + \frac{c\beta}{V} \Delta S^0 \right) + \frac{c^2 \alpha \beta}{V^2} \Delta S^0 \Delta T^0 - \left( \frac{\Phi^0}{V} + \frac{c\beta}{V} \Delta S^0 \right) \left( -\frac{\Phi^0}{V} + \frac{c\alpha}{V} \Delta T^0 \right) \right\}. \quad (26)$$

We have restricted our analysis to a range of basic states where the bracket [...] is negative. Positive values correspond to basic states that are not realized in the present climate, viz., a reversed thermohaline cell or a small ratio of meridional salinity gradient to meridional temperature gradi-

ent. For mixed boundary conditions (fixed atmospheric temperature and fresh water flux) the range of basic states considered is characterized by

$$0.5 < \frac{\beta \Delta S^0}{\alpha \Delta T^0} < 1. \quad (27)$$

For this range, the stability condition (26) always fails for mixed boundary conditions. A freshwater perturbation at high latitudes changes the density and reduces the northward salt transport, which amplifies the decrease in density and leads to a "polar halocline catastrophe". Our finding of an unstable THC under mixed boundary conditions with respect to infinitesimal changes in high latitude salinity is consistent with earlier results from 2-D models of Marotzke et al. (1988) and Marotzke (1990) and a 3-D model of Weaver and Sarachik (1991). In other models using mixed boundary conditions (Bryan, 1986), finite amplitude perturbations may be necessary to initiate a transition for which the ocean becomes unstable. The sensitivity of the THC under mixed boundary conditions is influenced by the meridional salinity difference  $\Delta S^0$  resulting from the strength of the fresh water flux forcing (Weaver et al., 1991) which is consistent with (27). All ocean models under mixed boundary conditions show a very high sensitivity against sea surface salinity perturbations at high latitudes.

Since the real climate system is less sensitive to these perturbations, there must be at least one neglected negative feedback to stabilizes the climate system. When the meridional mass transport is reduced due to a salinity anomaly at high latitudes, the atmosphere will be cooled by a reduced heat flux from the ocean. Deep water formation can still take place at a reduced rate with fresher but colder water. In our coupled system with the above-estimated values of  $K$  and  $K_2$ , we found that the right hand side of (26) is 0.57 which is less than the value for  $\varepsilon$  estimated by (23). Therefore, this system is stable with respect to infinitesimal perturbations in high latitude salinity. However, with another choice of the transport parameters  $K$  and  $K_2$  the system can be closer to the bifurcation point at which the system becomes unstable. To show the effect of different transport parameters, the stability condition (26) is calculated and plotted in the parameter space ( $K_2$ ,  $K$ ) in Fig. 2 (solid line). Increasing the meridional atmospheric transports of heat and moisture

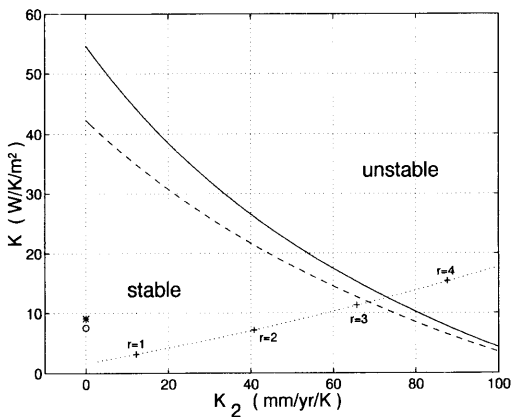


Fig. 2. Stability diagram in the parameter space for the eddy coefficient of heat transport  $K$  and the sensitivity coefficient of the hydrological cycle  $K_2$ , which is defined by:  $\delta(P - E) = -K_2 \delta T_A^{\text{HL}}$ . The coupled system is linearly stable below the curve and unstable above. The solid line and the pair of coefficients, marked by (+) lying on the dotted curve, correspond to our coupled system for different power laws with exponent  $r$ . With the estimated parameters  $(K_2, K)$ , our coupled system is stable with respect to small perturbations in high latitude salinity until  $r \leq 3.3$ . The dashed line corresponds to the parameters  $(Q_2, B) = (46 \text{ W m}^{-2} \text{ K}^{-1}, 3 \text{ W m}^{-2} \text{ K}^{-1})$ , which may be compared with the values of Stocker et al. (1992), marked by (\*), and Rahmstorf and Willebrand (1995), marked by (O).

(increasing  $K_2$  and  $K$ ) destabilizes the system. Enhanced eddy activity brings more warm and humid air to regions where deep water formation takes place and reduces the density of the surface water. Note that a higher power law for the eddy heat transports destabilizes the system. With our choice of parameters the system is linearly unstable above  $r = 3.3$  (Fig. 2). The stability appears to be sensitive to both heat and fresh water flux changes through eddy activity. Changes of the fresh water flux act as a strong destabilizing feedback. For a negative temperature anomaly considered, the temperature dependent part of  $\delta F_1$  in (12) reduces the latent heat transport and the destabilizing effect of the atmospheric heat transport and fresh water flux. However, the effect of the hydrological cycle is a great uncertainty and must be studied quantitatively by complex climate models.

Fixing the atmospheric temperature under mixed boundary conditions could be interpreted formally as an atmosphere with a poleward heat

transport being so effective that the atmosphere temperature remains unchanged. For mixed boundary conditions, the heat flux rates  $Q_2$  and  $Q'_2$  in (25) are used to calculate an equivalent coefficient  $(BK)_{\text{equiv}}$  that can be compared with  $B + K(1 - \eta)$  of our model:

$$(BK)_{\text{equiv}} = \frac{Q_2 Q'_2}{Q_2 - Q'_2}. \quad (28)$$

The transport quantity  $(BK)_{\text{equiv}}$  in eq. (28) is infinite under mixed boundary conditions with  $Q_2 = Q'_2$ . In terms of our model that system belongs to the unstable region at the  $K_2 = 0$  axis in Fig. 2.

According to condition (26), the stability of the coupled system (19, 20) depends on the basic state  $(\Delta T^0, \Delta S^0)$ . We analyze the sensitivity with respect to the basic state, fixing the transport coefficients  $(K_2, K)$  at our previous estimates. The present circulation is characterized by a temperature-controlled deep water formation with a strong overturning stream function  $\Phi^0$ . The corresponding basic state  $(\Delta T^0, \Delta S^0) = (-13.5 \text{ K}, -1.5 \text{ psu})$  with  $c = 17 \cdot 10^6 \text{ m}^3 \text{ s}^{-1}$  is stable for high latitude salinity perturbations (Fig. 3). Furthermore, we find

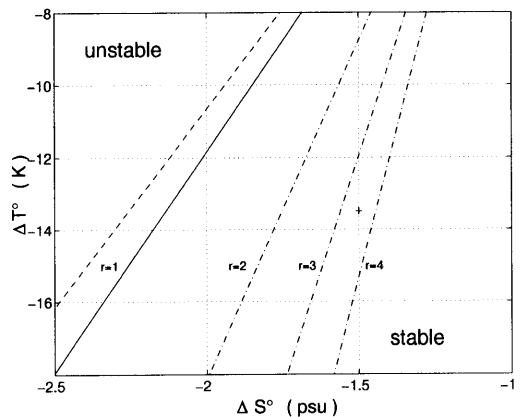


Fig. 3. Stability diagram in the parameter space  $(\Delta T^0, \Delta S^0)$  with fixed transport parameters  $(K_2, K)$ . The coupled system is linearly stable below the curve and unstable above. The dashed and solid lines correspond to a linear diffusion ( $r = 1$ ) for the atmospheric transports while the dashed dotted lines correspond to higher power laws. A strong thermally dominated deep water formation and small salinity differences  $\Delta S^0$  favor the stability of the THC. An enhanced overturning rate (by increasing the parameter  $c$  by 20%; dashed line) shifts the line of critical stability upwards.

Table 1. Comparison of different experiments in the literature

Lit.	BC	$\phi_0$ (Sv)	$\left(\frac{Q_2}{W}\right)$ $\left(\frac{1}{m^2K}\right)$	$\left(\frac{B}{W}\right)$ $\left(\frac{1}{m^2K}\right)$	$\left(\frac{K}{W}\right)$ $\left(\frac{1}{m^2K}\right)$	$\left(\frac{K_2}{mm}\right)$ $\left(\frac{1}{yrK}\right)$	$Q_2(1-\varepsilon)$ $\left(\frac{W}{m^2K}\right)$	$\varepsilon$
Box ( $r=1$ )	EBM	14	38	2	3.2	12	4.6	0.88
Box ( $r=2$ )	EBM	14	38	2	7.2	40	6.8	0.82
SWM	EBM	14	48.6	4.1	9.1	0	9.5	0.80
RW	EBM	13	46	3	7.6	0	8.7	0.81
NSM	EBM	7–10	100	1.7	ca. $Q_2/2$	70	ca. $Q_2/2$	0.5
LGC	EBM	–2	45	2.2	20	< 10	11.9	0.74
ZGL	SM	13	45	2.4	0	0	2.3	0.95
					(BK) <sub>equiv</sub>	$K_2$	$Q'_2$	$\varepsilon_{equiv}$
ZGL	mMBC	13	45	–	7.9, 5.1	0	6.8, 4.5	0.85, 0.9
MM	mMBC	17	40	–	168, 54, 0	0	27, 16, 0.4	0.3, 0.6, 1
PK	mMBC	22	61	–	284, 120, 0	0	41, 30, 0	0.3, 0.5, 1
B	MBC	20	97	–	$\infty$	0	97	0

The present study is denoted “Box”. All other values are estimated from the information given in the respective papers. For Rahmstorf and Willebrand (1995, RW in the table), the transport coefficient  $K$  is recalculated for the North Atlantic by assuming zonal homogeneity. The acronyms stand for: SWM for Stocker et al. (1992), NSM for Nakamura et al. (1994), LGC for Lohmann et al. (1995), ZGL for Zhang et al. (1993), MM for Mikolajewicz and Maier-Reimer (1994), PK for Power and Kleeman (1994), and B for Bryan (1986). Boundary conditions (BC) are abbreviated as EBM for energy balance model, SM for Schopf’s model and (m)MBC for (modified) mixed boundary conditions. For the boundary conditions EBM and SM, the parameter  $\varepsilon$  is calculated from (22), whereas for mixed boundary conditions,  $\varepsilon_{equiv}$  and (BK)<sub>equiv</sub> are calculated according to (25, 28). Note that Lohmann et al. (1995) consider a different basic state. In the other cases, the values of  $\varepsilon$  and  $K_2$  indicate roughly the sensitivity of the THC due to the boundary conditions.

that increasing the meridional overturning parameter  $c$  stabilizes the system by shifting the line of critical stability upwards in Fig. 3 (dashed line for an increase in  $c$  of 20%). Fig. 3 indicates that a different basic state with either a smaller meridional temperature gradient  $|\Delta T^0|$  or a larger salinity gradient  $|\Delta S^0|$  would be linearly unstable. Such a different basic state could for instance result from different greenhouse gas concentrations in the atmosphere which, according to coupled GCM results (Manabe and Stouffer, 1993), tend to produce a smaller temperature difference and a larger salinity contrast than presently observed. This climate state is connected with a decreased sensible heat transport and an increased latent heat trans-

port, partly compensating each other (Chen et al., 1995; Tang and Weaver, 1995).

However, we have not taken into account that in a warmer than today’s climate, e.g., the Eemian interglacial or a climate with higher greenhouse gas concentrations, the temperature dependence of latent heat transport would be larger (to be represented by a larger coefficient  $K_{11}$  in our model). For negative temperature anomalies in such a warmer climate the sensitivity coefficient of the hydrological cycle  $K_2$  in (18) would be reduced which again stabilizes slightly the system.

It is useful to compare different sensitivity studies in terms of the transport coefficients and heat flux rates of our box model. All experiments listed



in Table 1, except that of Lohmann et al. (1995), consider a thermally-dominated deep water formation. The values of  $\varepsilon$  and  $K_2$  roughly indicate the stability of the THC due to different boundary conditions. Mixed boundary conditions result in very unstable systems, as can be seen from the large transport coefficients  $(BK)_{\text{equiv}}$  and corresponding small values of  $\varepsilon_{\text{equiv}}$  (Bryan, 1986).

Zhang et al. (1993), Mikolajewicz and Maier-Reimer (1994) and Power and Kleeman (1994) consider a range of different time scales (24) and get a more stable system the longer the time scale. By increasing the time scales they mimic a non-zero  $K$  corresponding to  $(BK)_{\text{equiv}}$ . In Table 1, we denote this kind of boundary condition modified mixed boundary condition (mMBC).

An atmosphere without anomalous meridional heat transport, which corresponds to the case  $\varepsilon = \varepsilon_{\text{max}} = Q_2/(Q_2 + B)$  and  $(K_2, K) = (0, 0)$ , is Schopf's model (1983), which was used by Zhang et al. (1993) as the thermal boundary condition for their ocean model. Neglecting the destabilizing effect of the meridional heat transport, their resulting system was artificially stable with respect to perturbations in high latitude surface salinity.

Several investigations have included atmospheric transports with an EBM in a coupled ocean-atmosphere system. Transport coefficients  $(K_2, K)$  for some studies are recalculated for the North Atlantic domain (Table 1). Stocker et al. (1992) coupled a zonally averaged EBM to a zonally integrated ocean model. They found that the steady state depends on the assumptions about the zonal redistribution of precipitation. For the case of constant fresh water flux — otherwise  $K_2$  could be negative — the resulting parameters yield a system that is very well in the stable region of Fig. 2. This is partly a consequence of neglecting meridional transport of water vapour. Rahmstorf (1994) and Rahmstorf and Willebrand (1995) also neglect changes in the fresh water flux. Thus, their model also corresponds to points at the  $K_2 = 0$  axis in Fig. 2. The critical stability for their model parameters, calculated with (26), corresponds roughly to the dashed line in Fig. 2. The lower critical stability compared to our model is due to a larger heat flux rate. We find that for the EBMs of Table 1, values for  $\varepsilon$  are all similar, except for Nakamura et al. (1994) who admittedly overestimate the atmospheric heat transport due to their tuning. They consider a large catchment area

for the fresh water flux and find that the moisture feedback plays the important role in destabilizing the THC.

Our stability analysis shows that the less the heat flux is changed the more stable is the system, corresponding to high values of  $\varepsilon$ . Because the anomalous heat flux  $F'_{\text{oa}}$  in (21) is proportional to the heat flux rate  $Q_2$ , the line of critical stability in Fig. 2 (the dashed and solid lines) shifts downward as the heat flux rate  $Q_2$  is increased. However, in (21) we neglect changes of  $Q_2$ , denoted by  $\delta Q_2$ , which would give an additional term  $\delta Q_2(T - T_A^{\text{HL}})$  to the anomalous heat flux. Any physical process associated with high latitude salinity perturbations (e.g., enhanced surface wind

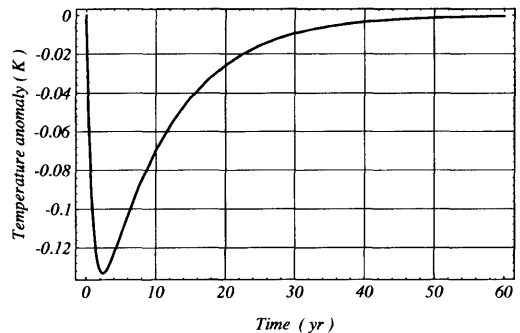


Fig. 4. Time series of salinity anomaly in the high latitude box. With parameters  $(K_2, K) = (12 \text{ mm yr}^{-1} \text{ K}^{-1}, 3.2 \text{ W m}^{-2} \text{ K}^{-1})$  for the meridional atmospheric transports of heat and moisture and  $r = 1$ , the system recovers from a perturbation in sea surface salinity of  $\delta S_{\text{GSA}} = 0.048 \text{ psu}$ .

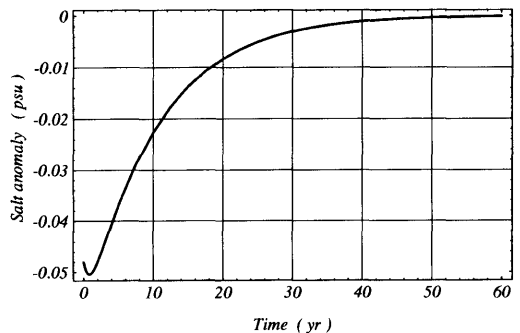


Fig. 5. Time series of sea surface temperature anomaly in the high latitude box perturbed with  $\delta S_{\text{GSA}} = 0.048 \text{ psu}$  at  $t = 0$  for the same experiment as Fig. 4.

speed) which increases the heat flux rate  $Q_2$  would reduce the anomalous heat flux  $|F'_{\text{oa}}|$  and with that the sensitivity of the system.

The remaining question for the coupled system is how large perturbations might cause a “polar halocline catastrophe”. For (19, 20) there is no easy Lyapunov function to estimate analytically the basin of attraction and the parameter dependency of that region. This is unfortunate because the linear part of the dynamics (19, 20) has a non-normal matrix, so that the condition (26) might be valid only in a very small neighborhood of the stable solution (Trefethen et al., 1993). Therefore, it is necessary to simulate the stability behavior for finite perturbations numerically. The great salinity anomaly (1968–1982) was characterized by a salt deficit in the upper few hundred meters in the North Atlantic estimated to be about  $7.2 \cdot 10^{13}$  kg by Dickson et al. (1988). In our polar box that deficit corresponds to a freshening of  $\delta S_{\text{GSA}} = 0.048$  psu. System (19, 20) is solved numerically for different salinity perturbations  $\delta S = n \times \delta S_{\text{GSA}}$ ,  $n = 1, 2, \dots$ . Figs. 4, 5 show time series of salinity and temperature for a perturbation of  $\delta S_{\text{GSA}}$  for the linear diffusion law ( $r = 1$ ). The initial increase of the salinity perturbation, as seen in Fig. 4, is due to the non-orthogonal stable manifolds. The relaxation times are given first by the (uncritical) eigenvalue with smaller real part and afterwards by the other, critical eigenvalue.

The coupled system with the above-estimated parameters remains stable for a salinity perturbation of  $\delta S \leq 13 \times \delta S_{\text{GSA}}$  for the linear diffusion law,  $5 \times \delta S_{\text{GSA}}$  for the quadratic power law and  $1 \times \delta S_{\text{GSA}}$  for  $r = 3$ . Time series for an initial salinity perturbation of  $5 \times \delta S_{\text{GSA}}$  for the quadratic power law are shown in Figs. 6, 7 and 8. Larger perturbations will lead to a different state of the non-linear system (19, 20) where the meridional mass transport vanishes (“polar halocline catastrophe”).

According to the linear stability analysis (Fig. 3), the critical salinity change  $(\Delta S^0)_{\text{crit}}$  of the basic state with an unchanged  $\Delta T^0$  is about  $-0.25$  psu for  $r = 2$ . The non-linear advection terms  $-(\Phi/V)\Delta T$  and  $-(\Phi/V)\Delta S$  of our dynamical system (1, 2) allows a larger critical perturbation  $\delta S_{\text{crit}}$  of  $-0.28$  psu which is about  $5 \times \delta S_{\text{GSA}}$  psu. Therefore, the non-linear oceanic transport terms of the system have a stabilizing effect on the THC.

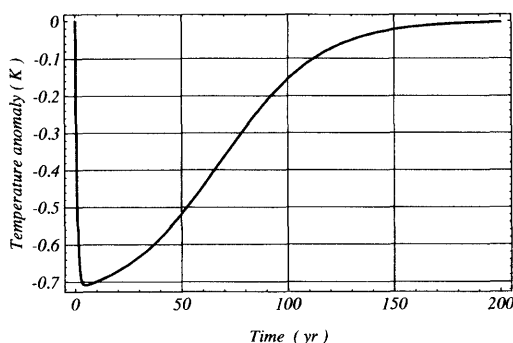


Fig. 6. Time series of surface salinity anomaly in the high latitude box after a perturbation of  $5 \times \delta S_{\text{GSA}}$  with a quadratic power law for the atmospheric transports.

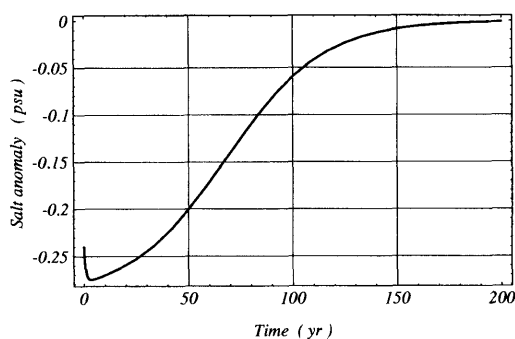


Fig. 7. Time series of sea surface temperature anomaly in the high latitude box after a perturbation of  $5 \times \delta S_{\text{GSA}}$  with a quadratic power law for the atmospheric transports.

#### 4. Conclusions

An understanding of feedback mechanisms in the coupled ocean-atmosphere system is obtained by a linear stability analysis. The dynamics of the atmosphere are simplified to a change of transport due to large-scale eddies, whereas the oceanic THC is approximated by a non-linear box model. In this coupled model, the qualitative effects of heat and fresh water fluxes on the THC are explored.

A strong, thermally-dominated deep water formation favors stability of the circulation with respect to salinity perturbations. The atmospheric transports of heat and moisture destabilize the THC, partly compensating for the stabilizing effect of a local atmospheric cooling due to reduced heat flux from the ocean to the atmosphere. In the

linearly stable region of the box model, there is a threshold of critical salinity perturbation beyond which the non-linear system becomes unstable.

Comparing box models like that of Nakamura et al. (1994) and the model presented in this paper with coupled EBM-OGCM models (Lohmann et al., 1995), it seems that box models are more sensitive to perturbations in surface fresh water fluxes at high latitudes than are GCMs. The case of the higher sensitivity likely lies in the coarse resolution of the box models and their simplified physics. The ocean circulation can easily be influenced by changes in the thermohaline surface conditions in deep water formation areas, whereas changes in other areas have little effect on the large-scale transports. Box models do not recognize the spatial structure imposed by rather localized sinking regions in the ocean. A logical next step is to study more complex coupled climate models to investigate the feedbacks identified in our model.

## 5. Acknowledgements

This research was partly funded by the "Deutscher Akademischer Austauschdienst", Germany. One author (G. Lohmann) would like to thank the Department of Physical Geography

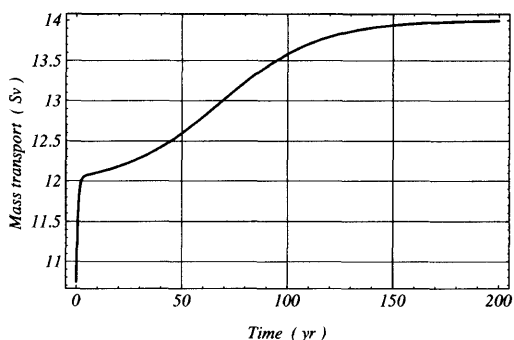


Fig. 8. Time series of the meridional mass transport  $\Phi$  (in  $\text{Sv} = 10^6 \text{ m}^3 \text{ s}^{-1}$ ) in the ocean according to (19, 20) with a quadratic power law for the atmospheric transports. The system is initialized with a surface salinity anomaly of  $5 \times \delta S_{\text{GSA}}$ . The system recovers from this perturbation and reaches the basic state with 14 Sv transport after 200 years.

at the University of Gothenburg, where part of this work was done, for a very friendly and fruitful stay. We thank Prof. Dr. Dirk Olbers and Prof. Dr. Sven Lindqvist for their support. We also thank Dr. Rebecca Woodgate for reviewing an earlier version of the manuscript. The manuscript benefited furthermore from comments of three anonymous reviewers. This is contribution number 966 from Alfred-Wegener-Institute for Polar and Marine Research.

## REFERENCES

- Birchfield, G. E. 1989. A coupled ocean-atmosphere climate model: temperature versus salinity effects on the thermohaline circulation. *Climate Dynamics* **4**, 57–71.
- Bolton, D. 1980. The computation of equivalent potential temperature. *Month. Weath. Rev.* **108**, 1046–1053.
- Branscome, L. E. 1983. A parameterization of transient eddy heat flux on a beta plane. *J. Atm. Sci.* **40**, 2508–2521.
- Bretherton, F. P. 1982. Ocean climate modeling. *Prog. Oceanogr.* **11**, 93–129.
- Broecker, W. S. and Peng, T.-H. 1989. The oceanic salt pump. Does it contribute to the glacial-interglacial difference in atmospheric  $\text{CO}_2$  content? *Global Biochem. Cycles* **3**, 215–239.
- Bryan, F. 1986. High latitude salinity effects and inter-hemispheric thermohaline circulations. *Nature* **323**, 301–304.
- Chen, D., Gerdes, R. and Lohmann, G. 1995. A 1-D atmospheric energy balance model developed for ocean modelling. *Theor. Appl. Climatol.* **51**, 25–38.
- Dickson, R. R. and Brown, J. 1994. The production of North Atlantic Deep Water: Sources, rates and pathways. *J. Geophys. Res.* **99** (C6), 12319–12341.
- Dickson, R. R., Meincke, J., Malmberg, S. A. and Lee, A. J. 1988. The "Great Salinity Anomaly" in the northern Atlantic 1968–1972. *Prog. Oceanogr.* **20**, 103–151.
- Green, J. S. A. 1970. Transport properties of large-scale eddies and the general circulation of the atmosphere. *Q. J. Roy. Meteor. Soc.* **96**, 157–185.
- Haney, R. L. 1971. Surface thermal boundary conditions for ocean circulation models. *J. Phys. Oceanogr.* **1**, 241–248.
- Keigwin, L. D., Jones, G. A., Lehmann, S. J. and Boyle, E. A. 1991. Deglacial meltwater discharge, North Atlantic deep circulation, and abrupt climate change. *J. Geophys. Res.* **96**, 16811–16826.
- Lohmann, G., Gerdes, R. and Chen, D. 1995. Sensitivity of the thermohaline circulation in coupled oceanic GCM-atmospheric EBM experiments. *Climate Dynamics*, in press.
- Maas, L. R. M. 1994. A simple model for the three-

- dimensional thermally and wind-driven ocean circulation. *Tellus* **46A**, 671–680.
- Manabe, S. and Stouffer, R. J. 1993. Century-scale effects of increased atmospheric CO<sub>2</sub> on the ocean-atmosphere system. *Nature* **364**, 215–218.
- Marotzke, J. 1990. *Instabilities and multiple equilibria of the thermohaline circulation*. PhD Thesis, Kiel University, 126 pp.
- Marotzke, J., Welander, P. and Willebrand, J. 1988. Instability and multiple steady states in a meridional-plane model of the thermohaline circulation. *Tellus* **40A**, 162–172.
- Mikolajewicz, U. and Maier-Reimer, E. 1994. Mixed boundary conditions in ocean general circulation models and their influence on the stability of the model's conveyor belt. *J. Geophys. Res.* **99** (C11), 22633–22644.
- Nakamura, M., Stone, P. H. and Marotzke, J. 1994. Destabilization of the thermohaline circulation by atmospheric eddy transports. *J. Climate* **7**, 1870–1882.
- Oberhuber, J. M. 1988. *An atlas based on the COADS data set. The budgets of heat, buoyancy and turbulence kinetic energy at the surface of the global ocean*. Max-Planck-Institute for Meteorology, Report No. 15.
- Oort, A. H. and Peixoto, J. P. 1983. Global angular momentum and energy balance requirements from observations. *Adv. Geophys.* **25**, 355–490.
- Power, S. B. and Kleeman, R. 1994. Surface heat flux parameterizations and the response of OGCMs to high latitude freshening. *Tellus* **46A**, 86–95.
- Rahmstorf, S. 1994. Rapid climate transitions in a coupled ocean-atmosphere model. *Nature* **372**, 82–85.
- Rahmstorf, S. and Willebrand, J. 1995. The role of the temperature feedback in stabilizing the thermohaline circulation. *J. Phys. Oceanogr.* **25**, 787–805.
- Sarnthein, M., Winn, K., Jung, S. J. A., Duplessy, J.-C., Labeyrie, L., Erlenkeuser, H. and Ganssen, G. 1994. Changes in east Atlantic deep water circulation over the last 30,000 years: Eight time slice reconstructions. *Palaeoceanogr.* **9**, 209–267.
- Schopf, P. S. 1983. On equatorial waves and El Nino. II: Effects of air-sea thermal coupling. *J. Phys. Oceanogr.* **21**, 1725–1739.
- Stocker, T. F., Wright, D. G. and Mysak, L. A. 1992. A zonally averaged, coupled ocean-atmosphere model for paleoclimate studies. *J. Climate* **5**, 773–797.
- Stommel, H. M. 1961. Thermohaline convection with two stable regimes of flow. *Tellus* **13**, 224–230.
- Stommel, H. M. 1993. A conjectural regulating mechanism for determining the thermohaline structure of the oceanic mixed layer. *J. Phys. Oceanogr.* **23**, 142–148.
- Stone, P. H. and Miller, D. A. 1980. Empirical relations between seasonal changes in meridional fluxes of heat. *J. Atm. Sci.* **37**, 1708–1721.
- Stone, P. H. and Yao, M. S. 1990. Development of a two-dimensional zonally averaged statistical-dynamical model. Part III. The parameterization of the eddy fluxes of heat and moisture. *J. Climate* **3**, 726–740.
- Tang, B. and Weaver, A. J. 1995. Climate stability as deduced from an idealized coupled atmosphere-ocean model. *Climate Dynamics* **11**, 141–150.
- Trefethen, L. N., Trefethen, A. E., Reddy, S. C. and Driscoll, T. A. 1993. Hydrodynamic stability without eigenvalues. *Science* **261**, 578–584.
- Weaver, A. J. and Sarachick, E. S. 1991. The role of mixed boundary conditions in numerical models of the ocean's climate. *J. Phys. Oceanogr.* **21**, 1470–1473.
- Weaver, A. J., Sarachick, E. S. and Marotzke, J. 1991. Freshwater flux forcing of decadal and interdecadal oceanic variability. *Nature* **353**, 836–838.
- Vallis, G. K. 1982. A statistical-dynamical climate model with a simple hydrological cycle. *Tellus* **34**, 211–227.
- Zaucker, F. and Broecker, W. S. 1992. The influence of atmospheric moisture transport on fresh water balance of the Atlantic drainage basin: General circulation model simulations and observations. *J. Geophys. Res.* **97**, 2765–2773.
- Zhang, S., Greatbatch, R. J. and Lin, C. A. 1993. A reexamination of the polar halocline catastrophe and implications for coupled ocean-atmosphere modeling. *J. Phys. Oceanogr.* **23**, 287–299.